

biochemicals to be analyzed in unprepared samples, very rapidly and with high specificity.

The rapid development of ambient MS likely will accelerate interest in miniature mass spectrometers. We can foresee handheld mass spectrometers equipped with DESI ion sources. The current trend in MS miniaturization is driven by the desire to perform in situ chemical analysis and facilitated in large measure by the development of small ion-trap analyzers, which have led to tandem mass spectrometers in the 10-kg (total system) weight range (36). These developments have been extended to instruments fitted with ambient ion sources, and a portable DESI ion-trap system based on a cylindrical ion-trap analyzer has been built. The drive toward miniature instruments, in parallel with the drive toward ambient mass spectrometers, has created technology that now allows ambient ionization methods to be used with instruments small enough to serve as personal mass spectrometers for individuals. It is likely that chemical measurements could be made soon by individuals with the ease with which, a generation ago, mathematical computational power became widely available with the development of the electronic calculator and the personal computer. Suitable ambient mass spectrometers would allow many of the environmental, pharmaceutical, and physiological measurements described in this article, and these could be of intense personal interest to individuals. The confluence

of ambient and miniature MS has the potential to change not just MS but the whole subject of analytical chemistry.

References and Notes

1. J. B. Fenn, M. Mann, C. K. Meng, S. F. Wong, C. M. Whitehouse, *Science* **246**, 64 (1989).
2. S. J. Pachuta, R. G. Cooks, *Chem. Rev.* **87**, 647 (1987).
3. M. Karas, F. Hillenkamp, *Anal. Chem.* **60**, 2299 (1988).
4. V. V. Laiko, M. A. Baldwin, A. L. Burlingame, *Anal. Chem.* **72**, 652 (2000).
5. Z. Takats, J. M. Wiseman, B. Gologan, R. G. Cooks, *Science* **306**, 471 (2004).
6. M. L. Pacholski, N. Winograd, *Chem. Rev.* **99**, 2977 (1999).
7. J. F. Mahoney *et al.*, *Rapid Commun. Mass Spectrom.* **5**, 441 (1991).
8. R. B. Cody, J. A. Laramée, H. D. Durst, *Anal. Chem.* **77**, 2297 (2005).
9. Z. Takats, I. Cotte-Rodriguez, N. Talaty, H. W. Chen, R. G. Cooks, *Chem. Commun.* 1950 (2005).
10. J. Shiea *et al.*, *Rapid Commun. Mass Spectrom.* **19**, 3701 (2005).
11. C. N. McEwen, R. G. McKay, B. S. Larsen, *Anal. Chem.* **77**, 7826 (2005).
12. I. Cotte-Rodriguez, Z. Takats, N. N. Talaty, H. Chen, R. G. Cooks, *Anal. Chem.* **77**, 6755 (2005).
13. Z. Takats, J. M. Wiseman, R. G. Cooks, *J. Mass Spectrom.* **40**, 1261 (2005).
14. M. Nefliu, A. Venter, R. G. Cooks, *Chem. Commun.*, 888 (2006).
15. M. Vincenti, R. G. Cooks, *Org. Mass Spectrom.* **23**, 317 (1988).
16. P. Kébarle, *J. Mass Spectrom.* **35**, 804 (2000).
17. H. Chen, N. Talaty, Z. Takats, R. G. Cooks, *Anal. Chem.* **77**, 6915 (2005).
18. S. Rodriguez-Cruz, *Rapid Commun. Mass Spectrom.* **20**, 53 (2005).
19. D. J. Weston, R. Bateman, I. D. Wilson, T. R. Wood, C. S. Creaser, *Anal. Chem.* **77**, 7572 (2005).
20. J. P. Williams, J. H. Scrivens, *Rapid Commun. Mass Spectrom.* **19**, 3643 (2005).
21. K. A. Hall, M. Green, P. Newton, F. Fernandez, paper presented at the 53rd American Society for Mass Spectrometry, San Antonio, TX, June 5–9 2005.
22. J. Henion, C. Van Pelt, T. Corso, G. Schultz, X. Huang, paper presented at the 53rd American Society for Mass Spectrometry, San Antonio, TX 2005.
23. L. A. Leuthold *et al.*, *Rapid Commun. Mass Spectrom.* **20**, 103 (2006).
24. G. J. Van Berkel, M. J. Ford, M. A. Deibel, *Anal. Chem.* **77**, 1207 (2005).
25. N. Talaty, Z. Takats, R. G. Cooks, *Analyst* **130**, 1624 (2005).
26. H. Chen, Z. Pan, N. Talaty, R. G. Cooks, D. Raftery, *Rapid Commun. Mass Spectrom.*, in press.
27. R. M. Caprioli, T. B. Farmer, J. Gile, *Anal. Chem.* **69**, 4751 (1997).
28. L. A. McDonnell *et al.*, *J. Mass Spectrom.* **40**, 160 (2005).
29. D. Touboul, F. Kollmer, E. Niehuis, A. Brunelle, O. Laprevote, *J. Am. Soc. Mass Spectrom.* **16**, 1608 (2005).
30. P. J. Todd, T. G. Schaaff, P. Chaurand, R. M. Caprioli, *J. Mass Spectrom.* **36**, 355 (2001).
31. J. M. Wiseman, S. M. Puolitaival, Z. Takats, R. M. Caprioli, R. G. Cooks, *Angew. Chem. Int. Ed.* **44**, 7094 (2005).
32. M. Nefliu, C. Moore, R. G. Cooks, in preparation.
33. H. Chen, I. Cotte-Rodriguez, R. G. Cooks, *Chem. Commun.*, in press.
34. J. A. Loo, *Mass Spectrom. Rev.* **16**, 1 (1997).
35. B. T. Ruotolo *et al.*, *Science* **310**, 1658 (2005).
36. L. Gao, Q. Song, R. G. Cooks, Z. Ouyang, in preparation.
37. This work was supported by grants from NSF, the Office of Naval Research, and ProSolia, Inc. (through the Indiana 21st Century Fund). We acknowledge the contributions of collaborators cited in the references.

10.1126/science.1119426

REVIEW

Probing Cellular Chemistry in Biological Systems with Microelectrodes

R. Mark Wightman

Over the past 20 years, the technological impediments to fabricating electrodes of micrometer dimensions have been largely overcome. These small electrodes can be readily applied to probe chemical events at the surface of tissues or individual biological cells; they can even be used to monitor concentration changes within intact animals. These measurements can be made on rapid time scales and with minimal perturbation of the system under study. Several recent applications have provided important insights into chemical processes at cells and in tissues. Examples include molecular flux measurements at the surface of single cells and through skin—which can offer insights into oxidative stress, exocytosis, and drug delivery—and real-time brain neurotransmitter monitoring in living rats, which reveals correlations between behavior and molecular events in the brain. Such findings can promote interdisciplinary collaborations and may lead to a broader understanding of the chemical aspects of biology.

Microelectrodes, sometimes termed ultramicroelectrodes, are chemical sensors with micrometer or smaller dimensions. Very small microelectrodes that report concentrations on the basis of potential changes across chemically selective mem-

branes at their tip, termed potentiometric electrodes, have been in use for decades. However, this review concerns voltammetric microelectrodes, microscopic devices that sense substances on the basis of their oxidation or reduction and that were introduced in the

early 1980s (1). More recently, voltammetric microelectrodes—dynamic devices that allow control of chemical environments as well as chemical sensing—have been used in a variety of unusual applications, including fabrication of microstructures and investigation of chemical fluctuations at the surface of single biological cells and in the living brain. They offer considerable advantages relative to voltammetric electrodes of conventional (millimeter) size. The small double-layer capacitance of microelectrodes enables chemical events occurring on the submicrosecond time scale to be monitored (2). Their small currents facilitate measurements in highly resistive media such as solvents without electrolyte and supercritical fluids (3). Unlike electrodes of conventional size, microelectrodes can be used in measurements on longer time scales, when the distance across which reactive molecules diffuse to the electrode is much greater than the electrode dimensions. Thus, very small electrodes can have markedly enhanced fluxes, which can enhance signal-to-noise ratios in trace metal ion determinations (1). In general, microelectrodes allow chemical measurements

Department of Chemistry, University of North Carolina at Chapel Hill, Chapel Hill, NC 27599, USA. E-mail: rmw@unc.edu

in spatial and temporal domains that were previously inaccessible.

When voltammetric microelectrodes were last reviewed in this journal, almost 20 years ago (4), researchers were still examining methods to construct them in different geometries. Today these methods are quite well developed. Fabrication of micrometer-sized electrodes can be as simple as sealing microwires or carbon fibers into a suitable insulator; alternatively, present-day lithographic techniques can be used to construct microelectrodes suitable for simultaneous electrochemistry and atomic force microscopy measurements (5). Methods for constructing electrodes with submicrometer dimensions were slower to develop but now are commonplace (6). The diffusional concepts are now well understood and are discussed fully in a textbook of electrochemistry (7). Today, much of the use of microelectrodes exploits their ability to explore chemistry in very small domains, especially those associated with biological systems. For example, microelectrodes can be coupled to a micropositioner that can be moved in three dimensions to provide a spatially resolved view of chemical events much like the physical characterization provided by other scanning probe microscopies. This approach, termed scanning electrochemical microscopy (SECM), was the subject of a recent monograph (8).

Although many interesting systems have been explored with microelectrodes, this review focuses on their use at single cells and in intact tissue, where considerable recent progress has been made.

Determining Molecular and Ionic Fluxes in Biological Systems

Ion and molecule transport are essential for the maintenance of homeostasis in biological systems. The small size of microelectrodes has allowed site-specific molecular flux measurements in biological systems ranging from single cells to intact tissue. A prime target has been molecular oxygen. Amperometric sensing of O_2 by its electroreduction at a membrane-covered

electrode with a surface area of a few square millimeters, the Clark electrode, is a well-established technique. Miniaturization of such an assembly to micrometer dimensions provides a way to measure O_2 flux with high spatial resolution. This technique has been used in suspensions of *Escherichia coli* to examine the effects of Ag^+ on the bacteria's respiration (9). Ag^+ initially increased the respiration rate because it uncoupled the respiratory chain.

When biological cells are under metabolic stress, various molecular fluxes adjust to remove the stress. For example, menadione is toxic to hepatocytes because it can diffuse into cells and generate reactive oxygen species (10).

are considerably different from those measured at cancer-prone fibroblasts. The latter generated greater amounts of O_2^- and H_2O_2 and smaller amounts of NO^+ and $ONOO$ relative to normal fibroblasts.

Microelectrodes can also be used with intact biological tissue. For example, microelectrodes have provided fundamental information on transdermal drug delivery in research that involved the collaboration of electrochemists with a pharmaceutical company. Applied electric fields affect transport of the drugs through the skin in two ways: They induce electro-osmotic flow to propel neutral and charged species, and they induce iontophoretic mass transport to modulate the

flux of charged species.

SECM was used to measure transport rates in hairless mouse skin (12, 13). The direction of electro-osmotic transport indicated that the skin has a negative charge at physiological pH. Electro-osmosis induced by an applied electric field enhanced the transport rate of hydroquinone, a neutral molecule (Fig. 1). Mass transport could be enhanced further for ions because of the additional migrational component to mass transport. The results revealed that the major sites for electro-osmotic transport of reagents are found at hair follicles that have a radius of 21 μm . This fundamental research demonstrating the nonuniformity of the molecular fluxes across skin was used by pharmacists to develop

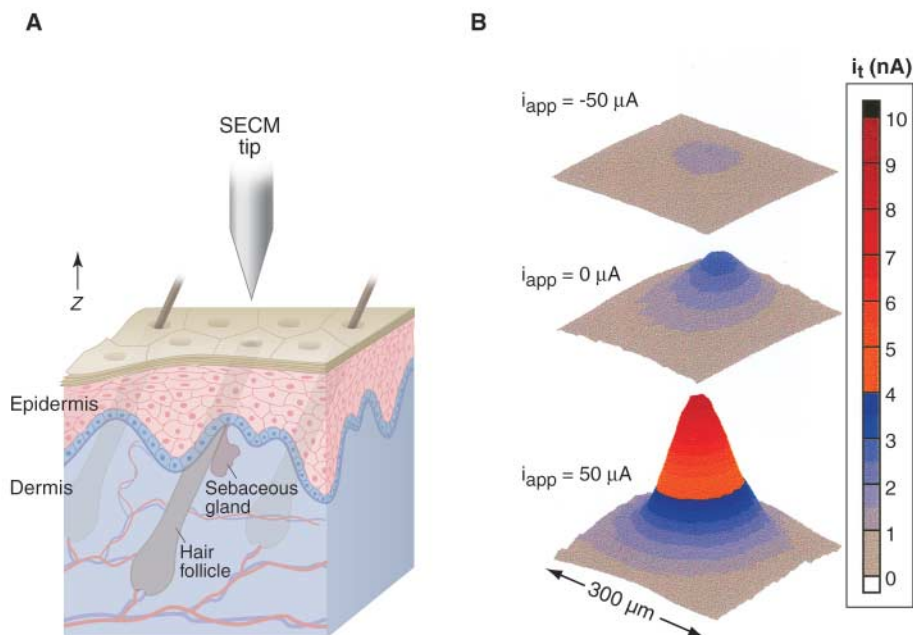


Fig. 1. (A) Schematic drawing illustrating the SECM tip positioned directly above the opening of a hair follicle. **(B)** SECM images of hydroquinone emerging from the opening of a hair follicle as a function of the applied iontophoretic current at pH = 6.0. The center image corresponds to diffusion of hydroquinone from the donor to receptor solutions without iontophoretic current. The lower image corresponds to positive iontophoretic current ($i_{app} = 50 \mu A$), inducing electro-osmotic flow in the same direction as diffusion. The upper image corresponds to a negative current ($i_{app} = -50 \mu A$), resulting in electro-osmotic flow opposing diffusion. A SECM tip of radius 2.6 μm , biased at 0.9 V versus Ag/AgCl, was used to record the images. Reprinted with permission from (13).

Within a cell, menadione is metabolized to the menadione-S-glutathione conjugate (thiodione) that is exported from the cell by an adenosine triphosphate-dependent pump. This pump-mediated efflux of thiodione was detected with a microelectrode by SECM both at single cells and at groups of highly confluent cells. The results quantified the flux of thiodione from a single cell. Oxidative stress causes increased generation of superoxide and nitric oxide derivatives, and these species can be individually monitored at the single cell level with a platinumized carbon-fiber microelectrode (11). The bursts of reactive species generated by fibroblasts from normal strains under oxidative stress

an FDA-approved drug delivery device for fentanyl, an opioid analgesic.

SECM has also been used to examine the flux of O_2 at different locations in bovine cartilage (14). Cartilage is composed of an extracellular matrix containing a gel of negatively charged proteoglycan molecules, specialized cells termed chondrocytes, and interstitial water, embedded in a porous supporting framework of collagen fibers. The microelectrode was placed within $\sim 1 \mu m$ of the surface of a cartilage sample that was immersed in solution. The topography of the cartilage was determined by monitoring the oxidation of $Ru(CN)_6^{4-}$ purposely added as an indicator molecule. This molecule does not

permeate the cartilage, and therefore fluctuations in the oxidation current during the positional scanning of the tip reflected the proximity of the surface. The topographic map of cartilage revealed depressions with diameters of 15 to 25 μm , which were attributed to chondrocytes because their distribution was similar to that observed with atomic force and light microscopy. Subsequent imaging of the same area of the cartilage sample for the flux of O_2 , again detected by its electroreduction, showed heterogeneous permeability of O_2 across the cartilage surface. The regions of high permeability were localized to the cellular and pericellular regions.

In the previous example of O_2 transport through cartilage, a concentration gradient was generated by the consumption of O_2 during its electroreduction, and the gradient induced the flux that was measured. However, within a living animal, O_2 flux is adjusted by fluctuations in blood flow, a process that is dynamically regulated by blood vessel dilation and constriction. In the brain, increased neuronal activity results in secretion of chemical messengers that cause blood vessels to dilate so that additional glucose is supplied to compensate for the increased metabolism. Positron emission tomography studies have shown that glucose metabolism becomes anaerobic during periods of high neuronal activity. Thus, during such periods, O_2 levels are predicted to increase in the extracellular fluid of the brain because of increased blood flow and decreased usage by oxidative metabolism (15).

With the use of a carbon-fiber microelectrode inserted into the rat striatum, this phenomenon could be directly observed after electrical stimulation of the medial forebrain bundle, a neuronal pathway into the striatum (16). The local O_2 concentration was measured with fast-scan cyclic voltammetry, using a voltage scan to negative potentials to detect O_2 and a positive scan to detect release of the neurotransmitter dopamine. The background subtraction procedure used with this technique also revealed pH changes, because they cause a shift in the background that leads to a differential alteration of the cyclic voltammograms. The O_2 increase and the basic pH shift induced by the stimulation both occurred a few seconds after neurotransmitter release, and their changes were inhibited by pharmacological agents known to attenuate vasodilation, such as adenosine-receptor antagonists and NO-synthase inhibitors. These O_2 and pH changes correlate in the living brain because carbon dioxide, a central component of the physiological pH buffering system, is removed by the increased blood flow. Similar changes did not occur in excised slices of brain tissue, even though neurotransmitter release is

still viable in this preparation, presumably because there was no blood flow.

Chemical Sensing at Individual Biological Cells During Exocytosis

Neurons and other cells communicate with each other through the triggered secretion of small molecules. A primary means by which these molecules are secreted is exocytosis, the regulated process in which a membrane-bound vesicle in the cytoplasm fuses with the plasma membrane via a Ca^{2+} -dependent mechanism. This fusion leads to the extrusion of the intravesicular contents, including the chemical mes-

senger. The approach is to use amperometry with a fixed applied potential while the current resulting from electrolysis of adjacent species is measured. A number of chemical messengers secreted by cells are electroactive and can be detected in this way. These include the catecholamines (dopamine, epinephrine, and norepinephrine), 5-hydroxytryptamine (5-HT or serotonin), and histamine. Peptides containing a tryptophan or tyrosine residue are also electroactive, as is nitric oxide. Alternatively, surface modification has been used for peptides such as insulin, whose detection by amperometry is facilitated by a ruthenium oxide coating (19). Because the secreted molecules detected are in the microscopic space between the electrode and the cell, all of the released contents are oxidized, yielding a quantitative measure of the number of molecules secreted per vesicle (20). An alternate method that provides the identity of the species detected is cyclic voltammetry (21). In this technique, the current is measured while the applied potential is swept over a range of interest.

A variety of evidence has established that the spikes observed upon stimulation of a secretory cell (Fig. 2) are of vesicular origin. They occur only after stimulation that promotes an elevated intracellular Ca^{2+} concentration, and they originate from spatially localized sites on the cell surface (18). In contrast, efflux of a predominantly non-vesicular component, ascorbate, is observed as a broad envelope rather than a discrete spike. Taken together, these measurements confirmed the quantal nature of chemical release by exocytosis. This approach was later used to measure exocytosis from a variety of cells (18) including mast cells from the immune system, immortal neuronal-like cells, insulin-secreting β cells from the pancreas, and invertebrate and mammalian neurons (22). In mammalian neurons, the amounts released from each vesicle are fewer than 50,000 molecules, so high-sensitivity recordings are required (Fig. 2).

This technique is noninvasive because measurements are made exterior to the cell. When the microelectrode is used with SECM, a map of the cell can be obtained and release sites across the cell surface can be probed (23, 24). Alternatively, very small (micrometer or smaller) electrodes can be used to spatially resolve exocytosis from well-defined regions of a single cell. With the use of a sensor incorporating four microelectrodes, the location of release sites on bovine chromaffin cells can be continuously monitored (25). Access to the interior of the cell can be achieved with a patch-clamp pipette containing a microelectrode, allowing recordings of the cytoplasmic levels of chemical messengers (26).

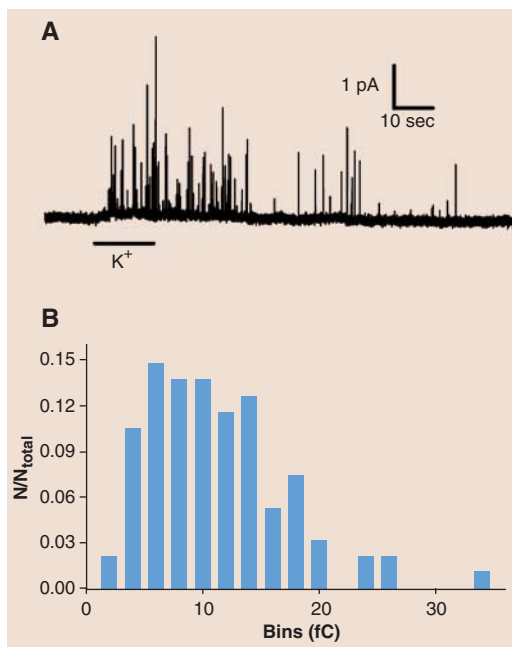


Fig. 2. Exocytotic current spikes from dopaminergic neurons isolated from mouse retina. (A) Application of an elevated K^+ solution depolarizes the cell membrane and results in a series of sharp amperometric spikes, each corresponding to a single exocytotic event. (B) Histogram of the distribution of charges of the spikes in (A); bins are in units of femtocoulombs. Reprinted with permission from (22).

sengers, into the extracellular space (17). This concept is thought to be governed by the quantal hypothesis, which asserts that chemical transmitters are stored and released in predetermined unit amounts that are independent of the event initiating release. Measurements with microelectrodes provided chemical evidence that directly demonstrated the outcome of exocytosis.

Because the size of carbon-fiber microelectrodes is similar to that of many biological cells, they are well suited to examine the chemical and temporal characteristics of secretory events at the cell surface (18). With the use of a micropositioner mounted on a microscope stage, the microelectrode can be placed directly in contact with the cell to monitor secretion. The simplest ap-

Microelectrode recordings at single cells have exposed a number of previously unknown features of exocytosis. In many cells with large vesicles (vesicle radius >100 nm), especially those with dense core vesicles, individual secretory events are prolonged relative to the time scale expected for simple diffusional dispersion, and vesicle extrusion is dominated by the time course needed for dissociation of the vesicle contents (27). At neurons (vesicle radius ~ 25 nm) as well as cells with large vesicles, the secretory packets are not quantized in a tight fashion (Fig. 2, for example). Rather, a broad distribution is found for the amounts released by exocytosis (18). Furthermore, quantal size can be adjusted pharmacologically with a concomitant change in vesicle volume (28). Recordings at cells with large vesicles reveal, at the initial stages of some exocytotic release events, a “foot”-like feature that reflects diffusion of the vesicular contents through an initially formed fusion pore (29). The foot can be reproduced in liposome preparations composed of nanotubes connecting different compartments (30). This foot occasionally flickers, which implies that the fusion pore has a fluctuating diameter. Release from neurons shows several events that appear to flicker, which suggests repeated, partial exocytotic events from the same vesicle (31)—a process termed “kiss and run” exocytosis that may arise from opening and closing of the fusion pore.

Measuring Dopamine Neurotransmission During Behavior

The process of neurotransmission governs virtually all functional aspects of the nervous system, including the triggering of contraction at neuromuscular junctions, activation of emotional responses in the amygdala, and the processing of memories in the hippocampus. Within the intact brain, neurons release neurotransmitters by the exocytotic process that has been characterized with microelectrodes at isolated cells. The specific site of release is the synapse, a narrow (10 to 100 nm) space between neurons. Once released, the neurotransmitter diffuses to its receptors—membrane-bound proteins that can recognize the specific neurotransmitter. For catecholamines and 5-HT, these receptors are distributed throughout the extracellular space, and neurotransmission is not restricted to the synaptic region (32). The binding of a neurotransmitter to its receptor triggers specific intracellular processes (opening of an ion channel, activation of cyclic adenosine monophosphate, etc.) that lead to information transfer between neurons. Neurotransmitter lifetimes in the extracellular space are short because metabolism or cellular uptake rapidly restores neurotransmitter concentrations to their original low levels.

To monitor neurotransmission, a chemical sensor must provide information from the micrometer dimensions and the millisecond time scale over which communication occurs. Sensing also requires high chemical specificity to allow selective monitoring, as well as a sensitivity for the neurotransmitter that is similar to the affinity of its natural biological receptors, often in the nanomolar range. Carbon-fiber microelectrodes have many of the properties required for such sensing, and for some years they have been used to monitor neurotransmission in the brains

of living but anesthetized organisms (33). In these experiments, the animal is placed in a stereotaxic frame and the electrode is lowered through a hole drilled in the skull to the region of interest. Dopamine has been a popular target of such studies because it plays several roles in the brain (34). Normal dopamine functioning is essential for coordinated motor movement; the symptoms of Parkinson's disease arise because of a shortage of this neurotransmitter. In addition, dopamine is a neurotransmitter in the brain reward pathway. Many drugs of abuse such as cocaine and amphetamine, which can evoke profound behavioral changes, appear to tap into the brain reward circuitry through dopaminergic neurons.

Fast-scan cyclic voltammetry has been shown to offer the necessary chemical selectivity and temporal resolution for in vivo measurements of dopamine (34). As practiced today, a fast-scan (400 V/s) cyclic voltammogram is obtained at regular intervals (typically 100 ms). After subtraction of the background current, the voltammogram reveals the substance(s) that changed in concentration over the measurement period. Distinct voltammetric curves are obtained for 5-HT and the catecholamines relative to other documented interferences, allowing for their identification. Overlapping signals recorded within the brain are resolved by principal components regression using an appropriate calibration set (35). Limits of detection are typically ~ 20 nM for dopamine. As noted above, the technique can be used to monitor O_2 and pH changes simultaneously with dopamine.

A cyclic voltammetry study in rats revealed that dopamine was released during electrical depolarization of its neurons—a procedure that generates action potentials, the normal mode of intracellular information transfer. When the depolarization was terminated, release ceased and dopamine was cleared by the dopamine transporter (36). Amperometry provides better time resolution in these experiments, allowing a clearer view of the rapidity of dopamine uptake (half-time $t_{1/2} = 20$ to 40 ms) (37). The importance of the dopamine transporter was unequivocally established with genetic knockout technology: In mouse brains lacking the transporter, dopamine clearance took 100 times as long as in normal mice (38). The control of extracellular dopamine as a balance between release and uptake is similar throughout the striatum, an area composed of the caudate-putamen and nucleus accumbens, as well as other dopaminergic regions (prefrontal cortex, amygdala), although the specific rates of release and uptake are regionally specific. The measured rates are also sensitive to pharmacological

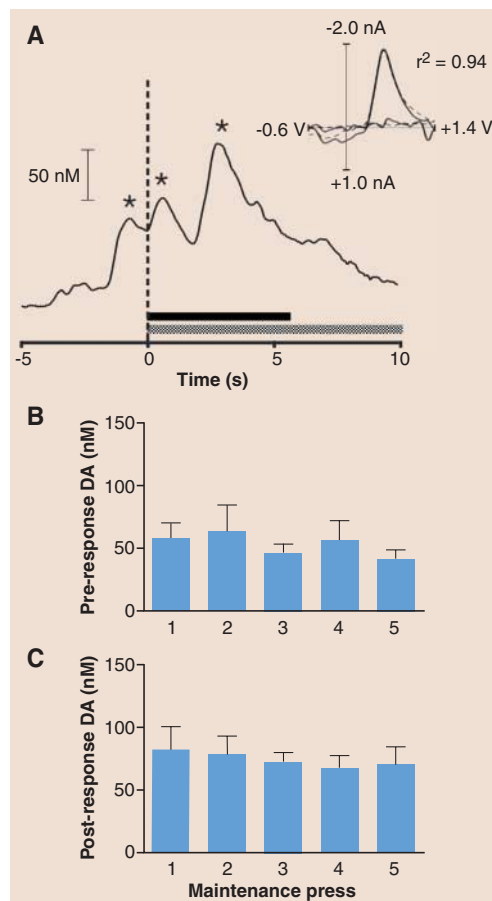


Fig. 3. Dopamine concentration in the rat nucleus accumbens at the time of the lever press for cocaine self-administration. (A) Pre- and postresponse dopamine transients associated with the operant response during a single trial. The lever press response occurs at $t = 0$, the black bar indicates the duration of the 0.33-mg cocaine infusion, and the shaded bar indicates the presentation of the drug-associated cues, which lasts for 20 s after the lever press response. Inset shows the cyclic voltammogram from the maximum dopamine change (solid line) compared to the voltammogram for electrically evoked dopamine release from the same animal. Linear regression analysis revealed a high correlation ($r^2 = 0.94$) between the voltammograms. (B and C) Mean (\pm SEM) prerespone (B) or postresponse (C) of dopamine concentrations during maintenance of cocaine self-administration. Data are from eight animals. Reprinted with permission from (40).

substances such as cocaine, amphetamine, and neuroleptic drugs, and the alterations in dopamine responses caused by these drugs reveal the chemical imbalances that they can generate.

Today the technology has advanced so that carbon-fiber microelectrodes can be used to measure dopamine concentration fluctuations in the brain during behavior. Working in collaboration with psychologists, voltammetrists have gleaned insights into the role of this neurotransmitter during reward-seeking. For example, in a rat trained to self-administer cocaine by pressing a lever, a dopamine transient occurs in the nucleus accumbens as the animal begins its approach to the lever (39). In addition, another dopamine transient occurs after the lever press in response to a cue (light and tone) that is associated with the lever press. These results can be seen on individual trials and remain constant in amplitude during repeated trials (Fig. 3). However, when the animal presses the lever but the cocaine is withheld, a protocol termed extinction, the dopamine transient associated with the cue diminishes in amplitude, even though the dopamine transients associated with approaching the lever remain (40). These dopamine fluctuations last for only a few seconds and so would be undetectable without the rapid chemical sampling that is provided by the microelectrode.

Although dopamine had long been implicated in reward-seeking as well as drug-taking, these results provide a high-resolution view of the specific role of this neurotransmitter in this well-characterized behavioral condition. For example, the findings during extinction suggest that dopamine transients encode the learned association between environmental cues and cocaine. Future investigations with this technology should enable probes of the role of dopamine in other behaviors such as learning and memory, as well as the role of 5-HT in sleep. However, such research requires close

interactions between chemists and psychologists to ensure the validity of the experimental design as well as appropriate interpretation of the results.

Conclusions

As is clear from the experiments summarized here, microelectrodes allow an unparalleled view of the dynamic chemical events that occur at the surface of cells and in intact tissue. These sensors allow for the observation of real-time chemical communication between neurons and of fundamental processes associated with oxidative metabolism. The results from these studies contribute to fields as diverse as drug delivery and neurochemical responses during substance abuse. Microelectrodes clearly enable interdisciplinary studies because they allow chemistry to be probed in unique microdomains in biological systems.

References and Notes

1. R. M. Wightman, D. O. Wipf, *Electroanal. Chem.* **15**, 267 (1989).
2. C. Amatore, E. Maisonhaute, *Anal. Chem.* **77**, 303A (2005).
3. N. Baltes, L. Thouin, C. Amatore, J. Heinze, *Angew. Chem. Int. Ed. Engl.* **43**, 1431 (2004).
4. R. M. Wightman, *Science* **240**, 415 (1988).
5. P. S. Dobson, J. M. R. Weaver, M. N. Holder, P. R. Unwin, J. V. Macpherson, *Anal. Chem.* **77**, 424 (2005).
6. B. Liu, J. P. Rolland, J. M. DeSimone, A. J. Bard, *Anal. Chem.* **77**, 3013 (2005).
7. A. J. Bard, L. R. Faulkner, *Electrochemical Methods, Fundamentals and Applications* (Wiley, New York, ed. 2, 2001).
8. M. V. Mirkin, A. J. Bard, *Scanning Electrochemical Microscopy* (Dekker, New York, 2001).
9. K. B. Holt, A. J. Bard, *Biochemistry* **44**, 13214 (2005).
10. J. Mauzeroll, A. J. Bard, O. Owghadian, T. J. Monks, *Proc. Natl. Acad. Sci. U.S.A.* **101**, 17582 (2004).
11. S. Arbault *et al.*, *Carcinogenesis* **25**, 509 (2004).
12. B. D. Bath, E. R. Scott, J. B. Phipps, H. S. White, *J. Pharm. Sci.* **89**, 1537 (2000).
13. B. D. Bath, H. S. White, E. R. Scott, *Pharm. Res.* **17**, 471 (2000).
14. M. Gonsalves *et al.*, *Biophys. J.* **78**, 1578 (2000).
15. N. K. Logothetis, B. A. Wandell, *Annu. Rev. Physiol.* **66**, 735 (2004).
16. B. J. Venton, D. J. Michael, R. M. Wightman, *J. Neurochem.* **84**, 373 (2003).
17. D. Sulzer, E. N. Pothos, *Rev. Neurosci.* **11**, 159 (2000).
18. E. R. Travis, R. M. Wightman, *Annu. Rev. Biophys. Biomol. Struct.* **27**, 77 (1998).
19. R. T. Kennedy, H. A. Lan, C. A. Aspinwall, *J. Am. Chem. Soc.* **118**, 1795 (1996).
20. R. M. Wightman *et al.*, *Proc. Natl. Acad. Sci. U.S.A.* **88**, 10754 (1991).
21. K. P. Troyer, R. M. Wightman, *J. Biol. Chem.* **277**, 29101 (2002).
22. S. E. Hochstetler, M. Puopolo, S. Gustincich, E. Raviola, R. M. Wightman, *Anal. Chem.* **72**, 489 (2000).
23. A. Hengstenberg, A. Blochl, I. D. Dietzel, W. Schuhmann, *Angew. Chem. Int. Ed. Engl.* **40**, 905 (2001).
24. J. M. Liebetrau *et al.*, *Anal. Chem.* **75**, 563 (2003).
25. I. Hafez *et al.*, *Proc. Natl. Acad. Sci. U.S.A.* **102**, 13879 (2005).
26. E. V. Mosharov, L. W. Gong, B. Khanna, D. Sulzer, M. Lindau, *J. Neurosci.* **23**, 5835 (2003).
27. C. Amatore, Y. Bouret, E. R. Travis, R. M. Wightman, *Angew. Chem. Int. Ed. Engl.* **39**, 1952 (2000).
28. T. L. Colliver, E. J. Hess, E. N. Pothos, D. Sulzer, A. G. Ewing, *J. Neurochem.* **74**, 1086 (2000).
29. R. H. Chow, L. Von Rüden, E. Neher, *Nature* **356**, 60 (1992).
30. A. S. Cans *et al.*, *Proc. Natl. Acad. Sci. U.S.A.* **100**, 400 (2003).
31. R. G. W. Staal, E. V. Mosharov, D. Sulzer, *Nat. Neurosci.* **7**, 341 (2004).
32. S. J. Cragg, M. E. Rice, *Trends Neurosci.* **27**, 270 (2004).
33. R. N. Adams, *Prog. Neurobiol.* **35**, 297 (1990).
34. R. M. Wightman, D. L. Robinson, *J. Neurochem.* **82**, 721 (2002).
35. M. L. Heien *et al.*, *Proc. Natl. Acad. Sci. U.S.A.* **102**, 10023 (2005).
36. B. J. Venton *et al.*, *J. Neurochem.* **87**, 1284 (2003).
37. A. N. Samaha, N. Mallet, S. M. Ferguson, F. Gonon, T. E. Robinson, *J. Neurosci.* **24**, 6362 (2004).
38. B. Giros, M. Jaber, S. R. Jones, R. M. Wightman, M. G. Caron, *Nature* **379**, 606 (1996).
39. P. E. Phillips, G. D. Stuber, M. L. Heien, R. M. Wightman, R. M. Carelli, *Nature* **422**, 614 (2003).
40. G. D. Stuber, R. M. Wightman, R. M. Carelli, *Neuron* **46**, 661 (2005).
41. Research in this laboratory concerning microelectrodes in biological systems has been supported by NIH grants NS 15841, NS 38879, and DA 10900.

10.1126/science.1120027